Available online at www.sciencedirect.com

ScienceDirect

Materials Today: Proceedings 4 (2017) 7011–7017

materialstoday: PROCEEDINGS

www.elsevier.com/locate/procedia

13th International Conference on Nanosciences & Nanotechnologies & 9th International Symposium on Flexible Organic Electronics

The analysis of the stress corrosion effects for H atom in the symmetrical tilt Ni Σ5 (012) grain boundary structure*

H. H. Kart[a,*], S. Ozdemir Kart[a] and T. Cagin[b]

[a]*Department of Physics, Pamukkale University Kinikli Campus, 20020, Denizli, Turkey*
[b]*Material Science and Engineering, Texas A&M University, Texas, TX 77845-3122, USA*

Abstract

We employ a first-principles total energy method based on density functional theory as implemented in the Vienna ab-initio simulation package (VASP) for a detailed analysis of the symmetrical tilt Ni Σ 5 (012) GB with H impurity atoms in the structure of Σ 5 (012) GB. The effects of H segregation at the Ni Σ 5 (012) GB are investigated in details. The main goal of this study is to perform the ab initio simulations for the Ni Σ 5 (012) GB including the various impurity atoms at GB level as well as pure grain boundary models of Ni Σ 5 (012) GB. The grains can either be pushed apart or pulled together depending on the size of the impurity and nature of the local relaxations. Fundamental understanding of stress-corrosion cracking in metals and alloys including various impurity atoms is important to develop a new-structural material. Our calculations are compatible with the other first principle calculations.

Selection and peer-review under responsibility of the Conference Committee Members of NANOTEXNOLOGY2016 (13th International Conference on Nanosciences & Nanotechnologies & 9th International Symposium on Flexible Organic Electronics).

Keywords: Nickel, density functional theory, stress corrosion cracking and grain boundary structure

1. Introduction

Grain boundary (GB) embrittlement in metals induced by impurity atoms has been known for a long time. Some structural and physical properties undergo drastic changes when impurity atoms, especially corrosive ones, are

* Corresponding author. Tel.: +90-2582963588; fax: +90-2582963535.
E-mail address: hkart@pau.edu.tr

Selection and peer-review under responsibility of the Conference Committee Members of NANOTEXNOLOGY2016 (13th International Conference on Nanosciences & Nanotechnologies & 9th International Symposium on Flexible Organic Electronics).

present in the vicinity of grain boundary [1-4]. Despite the continuing effort to clarify impurity atoms induced properties of the materials, the physical and chemical mechanism is still not understood. One approach to clarify the GB embrittlement is to calculate the segregation energy difference between a GB and a fracture free surface by using the Rice-Wang model [5]. This model allows to determine whether the type of the segregating impurity in GB is embrittler or a cohesion enhancer. This model has been applied to Fe and Ni GB's in some studies [6-8]. The second approach to clarify the GB embrittlement is to examine the response of a GB with impurity segregation under various tensile stresses. The ideal mechanical strength of materials is the stress required to force deformation or fracture by the elastic instability of its crystal lattice. The realistic strength of material has been scientific challenges for over 80 years [9]. In covalent materials, the behavior of both the electrons and atoms should be considered to comprehend the basic mechanism underlying the strain-stress and stain-energy relationship of the realistic materials. Ab initio calculations based on the density functional theory (DFT) has been applied to the ideal tensile or shear strengths of interface in metals [10,11]. More realistic ab initio calculations have been performed to study the tensile strength and mechanical behavior of bulk crystal [12-14]. Recently, this method has been successfully applied to single crystals [15-18] as well as several clean GB's [19-22]. Yamaguchi et al. [1,2] investigated the impurity-induced GB decohesion by impurity segregation in a Nickel-Sulfur system. The total energy and average stress are obtained for each level of extension. By iterating this cycle, it is possible to observe failure from the weakest point at some critical stress. We have also used DFT method to investigate the effects of sulfur and boron impurity atoms in Ni Σ 5 (012) in our previous studies [23,24].

Fundamental understanding of stress-corrosion cracking in metals and alloys including various impurity atoms is important to develop a new-structural material. Hence, in this work, we employ a first-principles total energy method based on density functional theory as implemented in the Vienna ab-initio simulation package (VASP) for a detailed analysis of the symmetrical tilt Ni Σ 5 (012) GB with H impurity atoms in the structure of Σ 5 (012) GB. The effects of H segregation at the Ni Σ 5 (012) GB are investigated in details.

2. Computational Method

The calculations have been carried out by using the Vienna *ab-initio* simulation package VASP [24-27] with the projector augmented wave (PAW) potentials [28-31] within generalized gradient approximation (GGA) [27]. Moreover, k-space sampling is performed by using a 2x2x1 Monkhorst Pack scheme for Brillouin-zone integration in all model systems. Kinetic energy cutoff is set as 280 eV for the plane wave basis set. The Methfessel-Paxton smearing method with 0.1 eV smearing width is used for the determination of partial occupancies for each wave function. Model system size varies from a pure 80 Ni atom face centered cubic (fcc) model system to GB systems including as many as additional 12 hydrojen atoms. The atomic positions, shape and volume of the model systems have been relaxed. a, b, and c correspond to the x, y and z axis, respectively. Lattice vectors for each model system used in this work have been optimized.

The computational unit cell as shown in Fig. 1 is used for modeling for a Ni Σ 5(012) symmetrical tilt GB containing 80 Ni atoms with hydrogen atoms in the interstitial positions. Lattice planes parallel to GB-plane in this unit cell are labeled as GB0, GB1, GB2… and GB10. There are four equivalent sites to place the hydrogen atoms on the GB0 which is parallel to xy plane. These sites are in the plane of GB0, and are called as the vacancy sites to place the impurity atoms. Stable absorption sites on a (012) model surface for Hydrogen atoms are not neighbor each other in the model systems. The distance between two GB0 sites is 3.52 Å, which is equal to the lattice constant of fcc Ni. The binding energy per one impurity atom in the GB with respect to the atomic gas state of impurity atoms, E_b^{GB}, is calculated by using below equation;

$$E_b^{GB}N_i = E_{tot}^{GB}(N_{Ni}, N_i) - N_i E_{tot}^{atom,i} - E_{tot}^{Bulk}(N_{Ni}^0)\frac{N_{Ni} - N_{Ni}^0}{Ni^0}. \quad (1)$$

Here, $E_{tot}^{GB}(N_{Ni}, N_i)$ refers to the calculated total energy of the GB unit cell including N_{Ni} nickel atoms and N_i impurity atoms. $E_{tot}^{atom,i}$ is the total energy of one isolated impurity atom, N_{Ni}^0 number of nickel atoms in clean GB bulk and bulk unit cells. The last term in the expression is to adjust the number of nickel atoms when impurity atoms are substituted for nickel atoms. The total energy of an isolated impurity atom can be calculated by using a large super-cell (10x11x12 in Å) with spin polarization. Symmetry breaking in these calculations is taken into account. $E_{tot}^{GB}(N_{Ni}^0)$ is the total energy of the GB system without any impurities and $E_{tot}^{Bulk}(N_{Ni}^0)$ is also total energy of the fcc bulk Ni system.

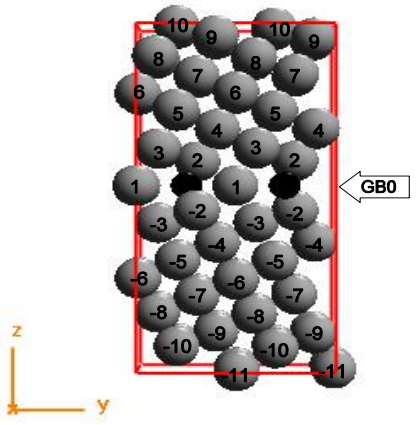

Fig. 1. Supercell structure of the model systems with 80 Ni-atoms in periodic boundary conditions containing a grain boundary (Σ 5 (012) symmetrical tilt GB). Gray balls indicate the Ni atoms and black balls represent the hydrogen atoms.

Segregation energy of the model systems studied in this work for different GB can be evaluated by using the equation [32]. This equation is given as;

$$\Delta E_{seg} = E_{tot}^{GB}(N_{Ni}, N_S) - E_b(bulk). \quad (2)$$

Here, $E_{tot}^{GB}(N_{Ni}, N_S)$ is the binding energy as stated above, and $E_b(bulk)$ is the binding energy when one H atom is in the inner bulk environment. In the $E_b(bulk)$ calculation, atomic geometries in the GB unit cell are changed to fcc symmetry in the whole cell.

3. Results and Discussion

Volume optimization of pure GB model system used in this work is performed by allowing the changes of the atomic positions, cell shape and cell volume. Optimization results for the a-, b- and c- vectors lengths and total energies for the model system are given in Table 1.

Table 1. The optimized/calculated lengths of a-, b- and c- vectors for pure GB model system.

	Optimize ions, volume and shape
a(Å)	6.481
b(Å)	8.317
c(Å)	16.512
TE(eV)	-431.305

We have done a series of calculations to determine the binding energies of atoms at different layers in order to assess the depth dependence in a given concentration for segregation. This is diligently accomplished by replacing a Ni atom at a given layer (0/6 through 6) with hydrogen atom. As shown in Table 2, the strongest binding energies are observed at the GB0 and GB0+GB2 layers. The orders of binding strengths at these two layers have similar magnitude. Schematic representation of models with one and four hydrogen atoms at GB0 level is shown in the Fig. 2. These figures are optimized structures obtained from ab initio calculations. Fig. 3a includes 6 hydrogen atoms at GB0 level while Fig. 3b contains 12 hydrogen atoms at GB0 level. Four hydrogen atoms are inserted to GB0 level while two hydrogen atoms are substituted for nickel atoms at GB2 level in the figure. Four hydrogen atoms are inserted to GB0 level and four impurity atoms are in the GB2 level as a substitution while the rest four atoms are inserted to the GB-2 level. Hydrogen atoms in GB2 and GB-2 levels are substituted in the place of nickel atoms. As shown in Fig. 3a and 3b, gray balls represent the nickel atoms and the blue atoms show the hydrogen atom. As shown in the figures, increasing the number of hydrogen atoms around the GB0 level causes the expansion of the GB. The distance between GB0 and GB1 or GB-1 layers clearly indicate the GB expansion in these model systems as the number of hydrogen atom increase around the GB.

The values for a-, b-, c- axis, cohesive energy (TE), total pressure (P_{tot}) and binding energy per hydrogen atom (E_b) are collected in the Table 2. Moreover, we have also presented some physical properties of model systems substituting one hydrogen atom in place of Ni atom at GBi (i=1,..6), as shown in Table 3. GB5 has the most cohesive energy while GB1 has the least cohesive energy as given in the Table 3.

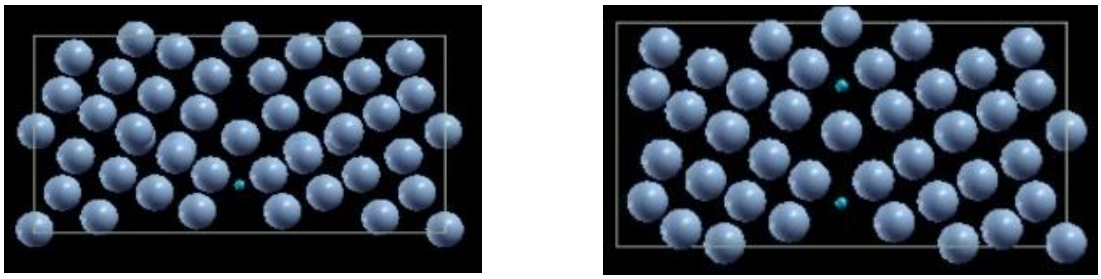

a) b)

Fig. 2. Schematically representation of models; a) containing one hydrogen atom at GB0, b) containing four hydrogen atoms at GB0 level. Gray balls in the figure represent the nickel atoms as the blue ones indicate the hydrogen atoms.

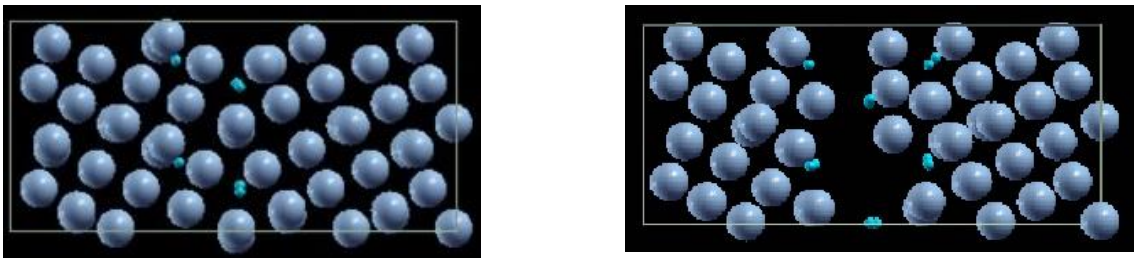

a) b)

Fig. 3. The model systems in a) and b) contain 6 and 12 hydrogen atoms, respectively. a) Four hydrogen atoms are inserted to GB0 level while two hydrogen atoms are substituted for nickel atoms at GB2 level in the figure. b) Four hydrogen atoms are inserted in GB0 level and four impurity atoms are in the GB2 level as a substitution while the rest four atoms are inserted to the GB-2 level. Hydrogen atoms in GB2 and GB-2 levels are substituted in the place of nickel atoms. Gray balls represent the nickel atoms and the blue atoms show the hydrogen atoms.

Table 2. Lattice constants (a, b, c) of the unit cell, total energy (TE), total pressure (P_{tot}), binding energy (E_b) for the model systems including hydrogen atoms at grain boundary layers and neighboring layers.

Layers	# of impurity atoms	a(Å)	b(Å)	c(Å)	TE(eV)	P_{tot}(kB)	E_b(eV)
GB0	1H	6.918	8.183	16.321	-433.825	0.59	-1.410
	2H	6.916	8.187	16.332	-437.515	0.32	-1.995
	3H	6.928	8.187	16.329	-440.683	-0.33	-2.016
	4H	6.920	8.194	16.352	-443.022	0.02	-1.819
GB0+GB2	5H	6.317	8.204	17.035	-441.620	-0.09	-2.034
	6H	6.298	8.214	17.913	-439.684	0.44	-1.188
GB0+GB2+ GB-2	12H	6.475	7.825	17.613	-421.173	-0.43	-1.651
GB2	1H	6.927	8.166	16.294	-427.219	-0.11	-0.212
	4H	6.394	8.231	16.209	-421.860	-6.93	-1.936

Table 3. Some physical properties of the model systems including one hydrogen atom at GBi (i=1,..6).

Layers	# of impurity atoms	a(Å)	b(Å)	c(Å)	TE(eV)	P_{tot}(kB)	E_b(eV)
GB1	1H	6.883	8.176	16.363	-425.783	-0.11	1.224
GB2	1H	6.927	8.166	16.294	-427.219	-0.11	-0.212
GB3	1H	6.920	8.163	16.338	-426.379	-1.37	0.628
GB4	1H	6.906	8.183	16.311	-426.484	-0.54	0.523
GB5	1H	6.934	8.174	16.276	-431.408	-0.29	-4.400
GB6	1H	6.897	8.174	16.349	-426.665	0.44	0.342

The distances between the GB0 and GBi (i=1,..6) levels are given in Table 4 when the GB0 and its neighboring levels of GB2 and GB-2 have various numbers of hydrogen atoms. It is obviously seen that the distances between the GB0 and other levels increase when more than 5 hydrogen atoms are added to GB0, GB2 and GB-2 layers. Distances for the model systems including any hydrogen atom are also given in the same table to observe the effect of hydrogen concentration on expansions between the GB0 and other layers.

Segregation energies (ΔE_{seg}) are calculated with respect to the number of layers by using Eq.2. and listed in Table 5. The segregation energy is determined for the model systems with one hydrogen atom at different layers which is defined as GBi (i=0,6).

As shown in Table 5, GB0, having minimum energy, is the most probable segregation layer. Yamagucgi et. al. [33] calculated grain boundary segregation energy of H atom in the GB0 level as -0.31 eV/H for the spin polarized state. As seen, our value of -1.22 eV/H for the GB0 level is compatible with the result reported in Ref. [33]. The difference between our result and their result may be due to the control parameters used in the calculations and the selected methods used in the calculations. The other layers such as 1, 2, 3, 4, 5 and 6 have higher segregation energies. As shown in Table 5, the highest value is shown in GB1 level.

It is shown that increasing number of hydrogen atoms in GB0 noticeably cause an increase in the segregation energy of the systems studied in this work. We have also checked the change of the segregation energy on account of hydrogen atoms to GB0 (for 1, 2, 3 and 4 hydrogen atoms), GB0+GB2 (for 5 and 6 hydrogen atoms) and GB0+GB2+GB-2 (for 12 hydrogen atoms). The calculated segregation energies decrease as hydrogen atoms are populated in GB0 layer. Moreover, further addition of hydrogen atoms to GB2 and GB-2 layers results in a noticeable increase in segregation energy. The calculated segregation energy values for GB0, GB0+GB2 and GB0+GB2+GB-2 are listed in Table 6.

Table 4: Distances between the GB0 level and GBi (i=1,..6) levels. Unit of the distance is given in terms of Å.

Distances (Å)	PURE	GB0-1H	GB0-2H	GB0-3H	GB0-4H	GB2+1H	GB2+4H	GB0-4H+ GB2-1H	GB0-4H+ GB2-2H	GB0-4H+ GB2-4H+GB2-4H
layer 1-layer 0	1.166	1.103	1.102	1.106	1.222	1.098	1.130	1.140	1.278	2.761
layer 2-layer 0	1.649	1.633	1.633	1.631	1.864	1.632	1.190	1.894	2.043	3.751
layer 3-layer 0	2.588	2.563	2.565	2.569	2.572	2.454	2.253	2.816	2.813	4.581
layer 4-layer 0	3.321	3.328	3.332	3.369	3.435	3.257	2.851	3.551	3.834	5.463
layer 5-layer 0	4.133	4.129	4.130	4.082	4.204	4.028	3.774	4.450	4.843	6.192
layer 6-layer 0	4.945	4.894	4.897	4.898	4.903	4.824	4.548	5.190	5.624	6.928

Table 5: Variation of segregation energy with respect to the number of layers. Segregation energy (ΔE_{seg}) is calculated while one hydrogen atom is included in the various layers. Segregation energy (ΔE_{seg}) values per hydrogen atom is given in the unit of eV/H.

	ΔE_{seg} (eV/H)
GB0+1H	-1.222
GB1+1H	6.820
GB2+1H	5.384
GB3+1H	6.224
GB4+1H	6.119
GB5+1H	1.195
GB6+1H	5.938

Table 6: Variations of segregation energy (ΔE_{seg}) values with various number of hydrogen atoms at different layers. Energy values are given in term of eV/H.

	ΔE_{seg} (eV/H)
GB0+1H	-1.222
GB0+2H	-2.456
GB0+3H	-2.693
GB0+4H	-2.605
GB0+4H+GB2+1H	-1.803
GB0+4H+GB2+2H	-1.180
GB0+4H+GB2+4H+GB-2+4H	0.953

4. Conclusion

We have investigated the effects of hydrogen impurity atoms on the Ni $\Sigma 5$ (012). The GB expansion is not shown when four impurity atoms are inserted in GB0 levels. This may be short-range attractive interaction which occurs between H atoms in Ni. When more H atoms are inserted in GB2 and GB-2 as well as GB0, the GB expansion is taken place. This expansion may be originated from the fact that Ni and H atoms form ordered alloy in the selected models. This phenomenon is usually explained by assuming the repulsive interaction between H atoms in Ni model systems. The origin of the repulsive force may be due to the H atoms prefer to bond with Ni atoms rather than with other H atoms. That is to say that, the repulsion between the H atoms occurs when many H atoms are squeezed in the small voids of the GB because of the Pauli principle. The binding energy of the H per atom evaluated from Eq. 1 and segregation energy of hydrogen per atom by using Eq. 2 at different layers show the same behavior as a function of layer number considered in this work. Segregation and binding energy for the hydrogen atoms show the two deep minima in GB0 and GB0+GB2 levels, indicating two the most probable segregation layer. The other layers such as

1, 2, 3, 4, 5 and 6 have similar segregation and binding energies. This work may be extended to investigate the effects of the impurity atoms such as Sulfur (S), Boron (B), and Oxygen (O) on the stress corrosion cracking for the metals of Ni, Al, and Fe with GB in the future.

5. Acknowledgements

Authors would like to thank the TUBITAK 2219 program for financial support of Dr. H. H. Kart to carry out the computer simulations at Texas A&M University and opportunity of project conducted in the Department of Physics supported by Pamukkale University (BAP Project No: 2016KKP206) .

6. References

[1] M. Yamaguchi, M. Shiga, H. Kaburaki, Science 307 (2005) 393–397.
[2] M. Yamaguchi, M. Shiga, H. Kaburaki, Science 309 (2005) 1677d.
[3] W.T. Geng, J.S. Wang, Science 309 (2005) 1677c.
[4] D. Mclean, Grain Boundaries in Metals, Oxford University Press, London, 1957.
[5] R. Rice and J. S. Wang, Mat. Sci. Eng. A 107 (1989) 23.
[6] R. Wu, A. J. Freeman, and G. B. Olsen, Science 265 (1994) 376.
[7] W. T. Geng, A. J. Freeman, R. Wu, C. B. Geller, and J. E. Raynolds, Phys. Rev. B 60 (1999) 7149.
[8] L. Zhong, R. Wu, A. J. Freeman, and G. B. Olsen, Phys. Rev. B 62 (2000) 13938.
[9] M. Sob L. G. Wang, V. Vitek, Comp. Mat. Sci. 8 (1997) 100.
[10] L. Goodwin, R. J. Needs, V. Heine**,** J. Phys.:Condens. Matter 2 (1990) 351
[11] T. Hong, J. R. Smith D. J. Srolovitz, Phys. Rev. B 47 (1993) 13615.
[12]Y. M. Huang, J. C. Spence, and O. F. Sankey, Phil. Mag. A 70 (1994) 53.
[13]M. Sob, L. G. Wang, V. Vitek, Mat. Sci. Eng. A 234 (1997) 1075.
[14]W. Li and T. Wang, Phys. Rev. B 59 (1999) 3993.
[15] G. L. Lu, Y. Zhang, S. Deng, T. Wang, M. Kohyama, R. Yamamoto, F. Liu, K. Horikawa, and M. Kanno, Phys. Rev. B 73 (2006) 224115.
[16] V. B. Deyirmenjian, V. Heine, M. C. Payne, V. Milman, R. M. Lynden-Gell, and M. W. Finnis, Phys. Rev. B 52 (1995) 15191.
[17] W. Li, and T. Wang, J. Phys.: Condens. Matter 10 (1998) 9889.
[18] S. Ogata, J. Li, and S. Yip, Science 298 (2002) 807.
[19] M. Kohyama, Phil. Mag. Lett. 79 (1999) 659.
[20] M. Kohyama, Phys. Rev. B 65 (2002) 184107.
[21]G: H. Lu, S. Deng, T. Wang, M. Kohyama, and R. Yamamoto, Phys. Rev. B 69 (2004) 134106.
[22] J. Chen, Y. –N. Xu, P. Rulis, L. Ouyang, and W. Y. Ching, Acta Mater. 53 (2005) 403..
[23] H. H. Kart, M. Uludoğan, T. Cagin, Comput. Mat. Sci. (2009) 1236-1242.
[24] H. H. Kart and T. Cagin, *Journal of Achievements in Materials and Manufacturing Engineering (JAMME)* 30 (2008) 177-181.
[25] G. Kresse and J. Hafner , Phys. Rev. B 49 (1994) 14251.
[26] G. Kresse and J. Furthmüller, Phys. Rev. B 54 (1996) 11169.
[27] G. Kresse and F. Furthmüller, Comput. Mat. Sci. 6 (1996) 15.
[28] P. E. Blöchl, Phys. Rev. B 50 (1994) 17953.
[29] G. Kresse and D. Joubert , Phys. Rev. B 59 (1999) 1758.
[30] J. P. Perdew, K. Burke and M. Ernzerhof, Phys. Rev. Lett. 77 (1996) 3865.
[31] J. P. Perdew, K. Burke, and M. Ernzerhof,.[Phys. Rev. Lett. 77 (1996) 3865], Phys. Rev. Lett. 78 (1997) 1396.
[32] D. Mclean, Grain Boundaries in Metals, Oxford Univ. Press, London , 1957.
[33] M. Yamaguchi, M. Shiga and H. Kaburaki, J. Phys.:Condens. Matter 16 (2004) 3933-3956.